

Computations of energy levels and wave functions of ground and excited states by the steepest-descent method

Ján Ftáčnik and Ivan Horváth

Department of Theoretical Physics, Comenius University, 842 15 Bratislava, Czechoslovakia

(Received 9 December 1988)

The steepest-descent method is used for the computation of energies and wave functions of ground and excited states of some simple quantum-mechanical systems. The accuracy of numerical results gives hope that the method can be used also in nonperturbative quantum-field-theory calculations. By calculating the evolution of the wave function along the steepest-descent path we are using the finite-element method.

I. INTRODUCTION

Some fundamental problems of particle physics, such as understanding the structure of the ground state of quantum chromodynamics and the structure of hadrons, require nonperturbative solutions for ground and excited states of field-theoretical systems. Completely satisfactory methods are not yet available, although some promising discrete schemes and variational strategies have recently been developed. These include among others the finite-element scheme studied in a series of papers by Bender, Milton, Sharp, and Strong,¹ t expansion by Horn and Weinstein,² and various versions of the Lanczos' variational tridiagonalization procedure.^{3,4}

In this paper we shall study in some detail possibilities offered by the steepest-descent method⁵ (SDM), which is the version of the variational method for calculation of ground and excited states of quantum systems. The calculations within the SDM are based on two equations. The former describes the motion of the state vector $|\psi\rangle$ in Hilbert space in the direction opposite to the gradient (steepest descent) of the expectation value $\langle\psi|\hat{H}|\psi\rangle$ of the Hamiltonian of the system. This version is suitable for the determination of the energy and state vector of the ground state of the system. The latter equation is somewhat more complicated and it describes the motion of the state vector in Hilbert space in the direction opposite to the gradient (steepest descent) of the dispersion of the energy $\langle\psi|(\hat{H}-\bar{H})^2|\psi\rangle$ with $\bar{H}=\langle\psi|\hat{H}|\psi\rangle$. The method converges to stationary states of the system, including excited ones.

In this paper we shall use the SDM to calculate energy levels and wave functions of some simple quantum-mechanical systems. In this way we intend to investigate the efficiency of the method and obtain the feeling of its applicability to more complicated systems. In practical applications of the SDM one has to describe the wave function of the system by a finite set of parameters. We have chosen to use the finite-element method which describes the wave function by the set of values on a grid of points and provides relatively accurate solutions for the evolution of the wave function in the direction opposite to the gradient in Hilbert space. Our choice of the finite-

element method (FEM) has been motivated mainly by successful applications of this method in discrete schemes developed by Bender *et al.*¹ It is, however, worth mentioning that the character of equations to be solved by using the FEM is rather different in the two cases. In the scheme by Bender *et al.*¹ one has to solve Heisenberg's equations for the time evolution of operators. These usually lead to coupled operator difference equations. The equations to be solved in the SDM are partial differential-integral equations with nonlinearities in their integral part and the FEM is thus used in rather non-standard situation.

We shall study here only one-dimensional systems for which the SDM gives very accurate results for both the ground and excited states. The results obtained indicate that the SDM has two characteristic features.

(i) It permits one to calculate energies and state vectors of excited states with roughly the same accuracy as in the case of the ground state.

(ii) The results for the ground state are to a large extent independent of the initial (trial) wave function in contrast to most of variational procedures in which the choice of the form of the trial wave function is a necessary prerequisite for obtaining accurate results. In what concerns computations of wave functions and energy levels of excited states, some preliminary rough information about the wave function is necessary since the expression $\langle\psi|(\hat{H}-\bar{H})^2|\psi\rangle$ has minima at all stationary states and the SDM leads the wave function to the closest minimum. We assume that these features will be preserved also in the case of higher-dimensional systems, but to substantiate this conjecture requires detailed studies and analyses of such systems.

The paper is organized as follows. In Secs. II and III we describe basic features of the steepest-descent and finite-element methods. The merging of these two methods is discussed in Sec. IV. Results of our numerical studies are described in Sec. V. Concluding comments are presented in Sec. VI and some technicalities are deferred to Appendices.

II. STEEPEST-DESCENT METHOD

Consider a system characterized by its Hamiltonian \hat{H} and choose a trial wave function $|\psi_{\text{in}}\rangle$ for its ground

state. The steepest-descent method⁵ for improving $|\psi_{in}\rangle$ is based on the fact that the expectation value

$$E(|\psi\rangle) = \frac{\langle \psi | \hat{H} | \psi \rangle}{\langle \psi | \psi \rangle} \quad (1)$$

attains its minimum in the ground state. The gradient of $E(|\psi\rangle)$ in Hilbert space is

$$\frac{\delta E(|\psi\rangle)}{\delta \langle \psi |} = \frac{1}{\langle \psi | \psi \rangle} \left[\hat{H} - \frac{\langle \psi | \hat{H} | \psi \rangle}{\langle \psi | \psi \rangle} \right] |\psi\rangle. \quad (2)$$

In order to improve the wave function in the fastest way possible, the wave function has to move in Hilbert space in the direction opposite to the gradient of $E(|\psi\rangle)$. Introducing an evolution parameter τ we thus obtain

$$\frac{\partial |\psi\rangle}{\partial \tau} = - \frac{1}{\langle \psi | \psi \rangle} \left[\hat{H} - \frac{\langle \psi | \hat{H} | \psi \rangle}{\langle \psi | \psi \rangle} \right] |\psi\rangle. \quad (3)$$

It is shown in Ref. 5 that this equation preserves the normalization of the wave function and thus for a normalized trial wave function $|\psi(\tau=0)\rangle \equiv |\psi_{in}\rangle$ we obtain a simplified equation

$$\frac{\partial |\psi(\tau)\rangle}{\partial \tau} = - [\hat{H} - \langle \psi | \hat{H} | \psi \rangle] |\psi(\tau)\rangle. \quad (4)$$

This equation leads asymptotically to the ground-state wave function $|\psi_{ground}\rangle$ provided that

$$\langle \psi_{in} | \psi_{ground} \rangle \neq 0. \quad (5)$$

The SDM equation for the evolution of the initial trial wave function to one of the excited state is based on the fact that the dispersion of the energy

$$D(|\psi\rangle) = \frac{\langle \psi | \hat{H}^2 | \psi \rangle}{\langle \psi | \psi \rangle} - \frac{\langle \psi | \hat{H} | \psi \rangle^2}{\langle \psi | \psi \rangle^2} \quad (6)$$

has a minimum in any of the stationary states of the system. The evolution equation for motion of $|\psi(\tau)\rangle$ to one of the stationary states is then given by making $\partial |\psi(\tau)\rangle / \partial \tau$ equal to the opposite of the gradient of $D(|\psi\rangle)$. The resulting equation preserves the normalization of the wave function and making use of this fact we obtain⁵

$$\frac{\partial |\psi(\tau)\rangle}{\partial \tau} = - (\hat{H}^2 - \langle \psi | \hat{H}^2 | \psi \rangle - 2 \langle \psi | \hat{H} | \psi \rangle \hat{H} + 2 \langle \psi | \hat{H} | \psi \rangle^2) |\psi(\tau)\rangle. \quad (7)$$

This equation is the starting point for our computation of energies and wave functions of excited states. As already pointed out Eq. (7) leads $|\psi_{in}\rangle$ to the "nearest" excited state. The resulting stationary state therefore depends on $|\psi_{in}\rangle$. In determining the energy and wave function of a particular excited state we have to be able to choose the initial wave function which is sufficiently close (in Hilbert space) to the wave function of the given stationary state. In quantum-mechanical problems this is frequently possible on the basis of known parity, number of zeros, etc.

III. FINITE-ELEMENT METHOD

The finite-element method (FEM) is an efficient numerical scheme for solving partial differential equations.⁶

The basic idea is quite simple. Suppose we have to find the solution $f = f(x, t)$ of the partial differential equation

$$F(x, t, \partial_x f, \partial_t f, \partial_{xx} f, \dots) = 0 \quad (8)$$

in region Ω , with specified boundary conditions. The region Ω is divided into a finite number of elements (subregions). In each of the elements the solution $f(x, t)$ is approximated by a polynomial in variables x, t , the degree of the polynomial depending on the problem studied. Coefficients of the polynomial in each of the elements are determined from conditions of two types: (i) The differential Eq. (8) is required to be satisfied at some points within the element; (ii) the continuity of the solution and of its derivatives is required in lattice points at the border of the element.

The total number of conditions is selected in such a way that conditions (i) and (ii) together with specified initial and boundary conditions determine completely the solution of the differential Eq. (8). The implementation of this general scheme to the solution of SDM equations will be described in the next section.

IV. MERGING OF THE STEEPEST-DESCENT AND FINITE-ELEMENT METHODS

We shall study here only simple quantum-mechanical systems with one degree of freedom. The wave function $|\psi\rangle$ is thus a function of the coordinate x : $\psi(x) \equiv \langle x | \psi \rangle$. In addition, wave functions in the SDM equations depend on the evolution parameter τ , to be called "time" in what follows. Our wave functions thus depend on two parameters $\psi = \psi(x, \tau)$.

The evolution Eqs. (4) and (7) can be rewritten as

$$\frac{\partial \psi}{\partial \tau} = - (\hat{H} - \bar{E}) \psi, \quad (9)$$

$$\frac{\partial \psi}{\partial \tau} = - [(\hat{H} - \bar{E})^2 - \bar{D}] \psi, \quad (10)$$

where $\bar{E} \equiv \bar{E}(\tau) = \int dx \psi^* \hat{H} \psi$; $\bar{D} \equiv \bar{D}(\tau) = \int dx \psi^* (\hat{H} - \bar{E})^2 \psi$ are the energy expectation value and its dispersion in the state $\psi(x, \tau)$. We are looking for solutions of Eqs. (9) and (10) for $\tau \geq 0$ and in particular for the limiting case $\tau \rightarrow \infty$ which corresponds to a ground state [Eq. (9)] or to one of the stationary states [Eq. (10)] of the system. For the harmonic oscillator and other systems where $-\infty < x < \infty$ the boundary condition is

$$\lim_{x \rightarrow -\infty} \Psi(x, \tau) = \lim_{x \rightarrow \infty} \Psi(x, \tau) = 0. \quad (11)$$

The trial wave function $\psi(x, 0) \equiv \phi_0$ is supposed to be normalized to one:

$$\int dx |\phi_0(x)|^2 = 1. \quad (12)$$

As the first step in using the FEM for solving Eqs. (9) and (10) we introduce a rectangular finite-element discretization with the time step s and the spatial step h (see Fig. 1). In the time direction we shall use linear finite elements

$$\psi_{n,m}(x, \tau) = \phi_{n,m}(x) + [\phi_{n+1,m}(x) - \phi_{n,m}(x)] \frac{\tau}{s}. \quad (13)$$

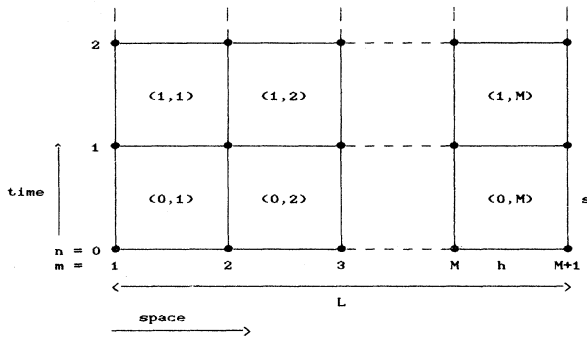


FIG. 1. Finite-element discretization. L is the spatial size of the region, M being the number of space elements; m numbers the space position of the element while n numbers the time coordinate of an element. An element is identified by indices of its left-hand corner (n, m) . Inside some of the elements we have indicated the corresponding symbol (n, m) .

In this way the function $\phi_{n,m}(x)$ is associated with the element (n, m) . The function $\phi_{n+1,m}(x)$ is associated with the $(n+1, m)$ element and Eq. (13) guarantees that $\psi_{n,m}(x, s) = \psi_{n+1,m}(x, 0)$. In this way the parametrization in Eq. (13) takes care of the continuity in the time variable.

In solving numerically Eq. (9) for the ground state of the system we parametrize the wave function in a given (n, m) element by a quadratic dependence on x . Taking into account Eq. (13) we then have

$$\begin{aligned} \psi_{n,m}(x, \tau) = & a_{n,m} \frac{x^2}{h^2} + b_{n,m} \frac{x}{h} + c_{n,m} \\ & + \left[(\bar{a}_{n,m} - a_{n,m}) \frac{x^2}{h^2} + (\bar{b}_{n,m} - b_{n,m}) \frac{x}{h} \right. \\ & \left. + \bar{c}_{n,m} - c_{n,m} \right] \frac{\tau}{s}. \end{aligned} \quad (14)$$

This form contains three free coefficients: $\bar{a}_{n,m}, \bar{b}_{n,m}, \bar{c}_{n,m}$, since the coefficients $a_{n,m}, b_{n,m}$, and $c_{n,m}$ have already been determined at the $(n-1)$ st "time" step. The coefficients $\bar{a}_{n,m}, \bar{b}_{n,m}$, and $\bar{c}_{n,m}$ are determined by three conditions: (i) the continuity of the function in the grid point $(n+1, m)$; (ii) the continuity of the derivative of the function in the same point; and (iii) the requirement that Eq. (9) is valid in the center of the (n, m) element. The situation is shown in Fig. 2.

Our computational scheme works in the following way. We construct the sequence of states $\phi_0, \phi_1, \dots, \phi_n, \dots$ (we have omitted here the spatial indices of the element) which correspond to the finite-element solutions of Eq. (9) in time levels $0, s, \dots, ns, \dots$. In this sequence each state improves the previous one. The detailed description of how the transition $\phi_n \rightarrow \phi_{n+1}$ was made is given in Appendix A.

The nonlinear and integral characters of Eq. (9) will reappear in condition (iii). It implies the nonlinear algebraic equation, in which all $3M$ coefficients $\bar{a}_{n,m}, \bar{b}_{n,m}, \bar{c}_{n,m}, m=1, 2, \dots, M$ are coupled. In this situation it is

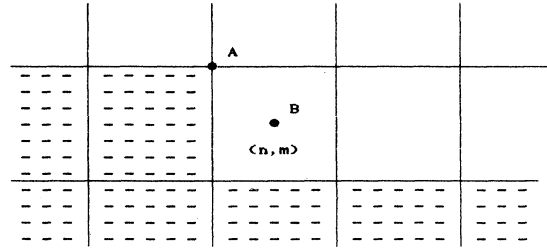


FIG. 2. Determination of coefficients $\bar{a}_{nm}, \bar{b}_{nm}, \bar{c}_{nm}$ the (n, m) element. The dotted region indicates parts in which the function $\Psi(x)$ is already known; two conditions are due to the continuity of the function and its derivative in the point A and the remaining condition comes from the differential equation being valid in the point B .

practically impossible to determine these coefficients and make the transition $\phi_n \rightarrow \phi_{n+1}$. It is necessary to replace Eq. (9) by the approximative one, the solution of which leads to the linear equations for coefficients. For this purpose we shall expand the solution of Eq. (9) for small τ . The result is

$$\begin{aligned} \psi(x, \tau) = & \phi_0(x) + \tau(\bar{E}_0 - \hat{H})\phi_0(x) \\ & + \frac{\tau^2}{2} [(\bar{E}_0 - \hat{H})^2 - 2\bar{D}_0]\phi_0(x) + O(\tau^3). \end{aligned} \quad (15)$$

Here, $\bar{E}_0 = \int dx \psi^* \hat{H} \psi$ and $\bar{D}_0 = \int dx \psi^* (\hat{H} - \bar{E})^2 \psi$ are the mean values of energy and its dispersion in the initial state $\psi(x, 0) = \phi_0(x)$. Using this expansion we obtain immediately

$$\bar{E}(\tau) = \int dx \psi^*(x, \tau) \hat{H} \psi(x, \tau) = \bar{E}_0 - 2\tau\bar{D}_0 + O(\tau^2). \quad (16)$$

Substitution into Eq. (9) leads to the linear equations for coefficients because $\bar{E}(\tau)$ is expressed only by the initial state $\phi_0(x)$. It is important to emphasize that this strategy is successful because our computational scheme accumulates almost no errors. Each transition $\phi_n \rightarrow \phi_{n+1}$ can be understood as the new problem of solution of Eq. (9) with the initial condition $\psi(x, 0) = \phi_n(x)$. This is how our scheme works. This approach and its modification is discussed in more detail in Appendix B.

In Eq. (10) for the excited states, the situation is quite analogous. This equation contains the operator \hat{H}^2 which involves the fourth derivative with respect to the spatial variable. That is why we have used the biquadratic spatial elements. The five coefficients of this approximation are determined by five conditions: (i)–(iv) the continuity of the function up to its third derivative in the grid point $(n+1, m)$ and (v) the requirement that Eq. (10) be satisfied in the center of the (n, m) element. It can be seen that the nonlinear character of Eq. (10) is even more peculiar than in the case of Eq. (9). The corresponding time expansion for the solution of Eq. (10), which we have used to express the mean values has the form

$$\psi(x, \tau) = \phi_0(x) + \tau[\bar{D}_0 - (\hat{H} - \bar{E}_0)^2] + O(\tau^2). \quad (17)$$

TABLE I. Ground-state energy of the particle in the infinite potential well [Eq. (9)]. M, N are the numbers of spatial elements and the time steps, respectively; s is the size of the time step. The size of the spatial region was $L=1$. Exact value: $\bar{E}=4.934802$.

| M | 5 | | | 20 | | |
|-----|--------|--------|--------|--------|--------|--------|
| s | 0.01 | 0.1 | 1 | 0.01 | 0.1 | 1 |
| 0 | 10.221 | 25.000 | 25.000 | 260.12 | 260.12 | 260.12 |
| 10 | 5.267 | 4.935 | 4.972 | 5.9009 | 4.9515 | 179.94 |
| 20 | 4.950 | | 4.971 | 4.9606 | 4.9367 | 104.05 |
| 30 | 4.936 | | | 4.9360 | 4.9353 | 77.20 |
| 40 | 4.935 | | | 4.9348 | 4.9351 | 49.52 |
| 50 | | | | | 4.9349 | 19.47 |
| 60 | | | | | | 4.9358 |
| 70 | | | | | | 4.9354 |

To conclude this section we shall give an argument which has led us to the requirement that the SDM equations (9) and (10) should be valid in the center of the element. Except for reasons of symmetry this choice was motivated as follows: Eqs. (9) and (10) are "correct" for the motion to the stationary state only if the initial state is normalized. The steepest-descent evolution then guarantees that the norm will be conserved: i.e.,

$$\frac{\partial}{\partial \tau} \int dx \psi^2 = 0 \quad (18)$$

or

$$\int dx \psi \frac{\partial \psi}{\partial \tau} = 0. \quad (19)$$

In terms of the discrete scheme which we are using the correctness of Eqs. (9) and (10), and the consistency by performing time steps is expressed by

$$\int dx \phi_n^2 = \int dx \phi_{n+1}^2 = 1. \quad (20)$$

Requiring that the equation is satisfied in points with time coordinate $\tau=as$, $0 \leq \alpha \leq 1$, we have, according to Eqs. (14) and (19),

$$(1-2\alpha) \int dx \phi_n \phi_{n+1} + \alpha \int dx \phi_n^2 - (1-\alpha) \int dx \phi_{n+1}^2 = 0. \quad (21)$$

It can be seen that by putting $\alpha=0.5$ we automatically satisfy condition (20). But even in this case the norm is not conserved exactly. In fact, Eq. (21) is only approximate because the SDM equation is not satisfied at all points with $\tau=as$. It is only satisfied at a finite number of them. That is why one would substitute the integrals in Eq. (21) by the integral sums. In both cases however Eq. (21) implies that the choice $\alpha=0.5$ is the optimal one. This result is very similar to that obtained by Bender *et al.*¹ in their finite-element scheme.

V. SOME SIMPLE SYSTEMS

A. Particle in an infinite square well

The Hamiltonian of the system is

$$\hat{H} = -\frac{\hbar^2}{2m} \frac{d^2}{dx^2}, \quad (22)$$

with explicit condition that $\psi(x) \equiv 0$ for $-\infty < x \leq 0$ and $L \leq x < \infty$. This is a very appropriate problem for the method developed here because the size of the spatial region (L) is given *a priori*.

We have solved Eq. (9) for the ground state. The rate

TABLE II. Ground state of the harmonic oscillator [Eq. (9)]. Dependence of the energy (\bar{E}) on the size of the spatial region (L) shows that the effective size of this region is about $L=5$. Exact value: $\bar{E}=0.5$.

| L | 1 | 5 | 10 |
|-----------|-------|-------|-------|
| \bar{E} | 4.961 | 0.506 | 0.514 |

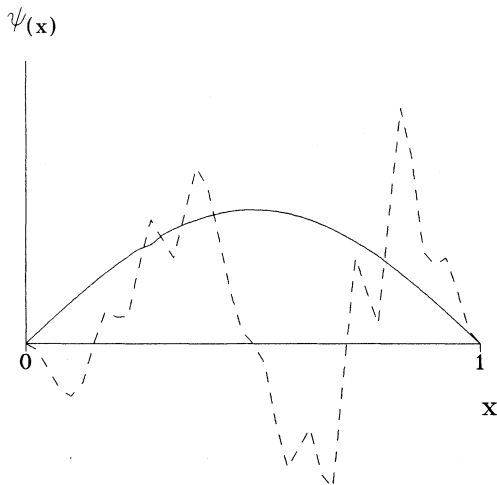


FIG. 3. Ground state of the particle in the infinite potential well. The dashed curve is the initial state with corresponding energy $\bar{E}=260.12$. The solid curve is the ground state, obtained after 15 time steps and its energy is $\bar{E}=4.9364$ (exact value: $\bar{E}=4.9348$).

TABLE III. Ground state of the harmonic oscillator [Eq. (9)]. M is the number of spatial elements. N is the number of time steps of size $s=0.5$. The size of the spatial region was $L=6$. Exact value: $\bar{E}=0.5$.

| $M \backslash N$ | 0 | 5 | 10 | 15 | 20 |
|------------------|---------|--------|--------|--------|-------|
| 5 | 3.580 | 0.907 | 0.508 | 0.505 | 0.505 |
| 10 | 9.3110 | 0.6701 | 0.5007 | 0.5007 | |
| 20 | 44.5417 | 0.5030 | 0.5004 | 0.5004 | |

of convergence in various situations is shown in Table I. The results were obtained with $\hbar^2/m=1$, $L=1$. It can be seen that by using only five spatial elements we have attained the accuracy 10^{-3} after a few "time steps" and by using 20 elements the accuracy becomes 10^{-4} . One can also notice that the region for a suitable choice of the time steps (s) is very large. This is closely connected with the fact that the steepest-descent equation is required to be valid in the center of the element. In this case the FEM is very accurate and it allows us to take such large time steps. It makes the method very flexible because one can always choose the interval L and the size of time and spatial steps s, h , which is optimal from the numerical point of view.

The values in Fig. 3 show that our computation of the ground state is rather independent of the choice of the wave function of the initial state. The dashed curve corresponds to the initial state with energy $\bar{E}=260.127$, the spatial structure of which is very different from the true wave function. After 15 time steps we have obtained the ground state with energy $\bar{E}=4.936$ (solid line) attaining the accuracy of 10^{-2} .

B. Harmonic oscillator

Our Hamiltonian will be

$$\hat{H} = -\frac{1}{2} \frac{d^2}{dx^2} + \frac{1}{2} x^2. \quad (23)$$

To perform our calculation the spatial interval must be chosen to be finite and sufficiently large. Noting that \hat{H} is symmetric with respect to $x \rightarrow -x$ we have chosen the finite region symmetric with respect to the origin. The optimal size L for this region can be found simply by trial and error. For instance, preliminary ground-state calcu-

lations lead to the values shown in Table II, depending on L . It can be seen that the effective size for the ground-state wave function is about $L=5$. Our calculations were done with $L=6$. The choice of even larger regions for calculations does not significantly improve the accuracy of the results. The results are given in Table III showing the time evolution of energy of the state, as it approaches the ground state.

The results of excited-state calculations are shown in Table IV. To calculate the n th state we have used an initial state of the form

$$\psi(x, 0) = \left[\frac{2}{L} \right]^{1/2} \sin \left[\frac{\pi n}{L} \left(x + \frac{L}{2} \right) \right], \quad (24)$$

which is the n th excited state of the Hamiltonian (22) with $(\hbar^2/m)=1$. For $n=2$ (first excited state) it is plotted in Fig. 4 together with the resulting excited-state wave function, obtained after 25 time steps.

Solving this system we have found some cases in which the transition $\phi_n \rightarrow \phi_{n+1}$ was numerically ill conditioned. This has led to the divergence in time evolution. In such cases one simply changes the values of h, s, L . From this point of view it is useful that the time steps s can be changed within a large interval of values.

C. Anharmonic oscillator

The Hamiltonian that describes this system is

$$\hat{H}(\lambda) = -\frac{1}{2} \frac{d^2}{dx^2} + \frac{1}{2} x^2 + \lambda x^4, \quad (25)$$

where λ is a parameter. For large λ (25) is a typical non-perturbative problem. Using the SDM leads to a situation which is analogous to previous cases.

TABLE IV. Ground- and excited-state energies of the harmonic oscillator [Eq. (10)]. M, N are the numbers of spatial elements and time steps, respectively, L being the size of the spatial region. \bar{D} is the value of variance in the resulting states. \bar{E} is the energy of the state and \bar{E}' its exact value.

| NS | 1 | 2 | 3 | 4 | 5 |
|------------|-----------------------|-----------------------|-----------------------|-----------------------|--------|
| L | 7 | 8 | 8 | 8 | 9 |
| M | 14 | 14 | 16 | 16 | 16 |
| N | 15 | 25 | 20 | 15 | 25 |
| \bar{D} | 0.88×10^{-3} | 0.30×10^{-2} | 0.13×10^{-1} | 0.59×10^{-1} | 0.11 |
| \bar{E} | 0.5001 | 1.5001 | 2.5036 | 3.5103 | 4.5320 |
| \bar{E}' | 0.5000 | 1.5000 | 2.5000 | 3.5000 | 4.5000 |

TABLE V. Ground state of the anharmonic oscillator [Eq. (9)]. For a given value of parameter λ the energy of the ground state (\bar{E}) is shown and compared with the value given in the literature (\bar{E}')⁷. L is the size of the spatial region and N is the number of time steps. The number of spatial elements was equal to $L=8$.

| λ | 0.1 | 0.2 | 0.4 | 1 | 10 | 100 | 1000 |
|------------|--------|--------|--------|--------|--------|--------|--------|
| L | 3.0 | 3.0 | 3.0 | 2.5 | 2.0 | 1.5 | 1.0 |
| N | 10 | 5 | 10 | 5 | 10 | 35 | 25 |
| \bar{E} | 0.5592 | 0.6026 | 0.6689 | 0.8039 | 1.5057 | 3.1434 | 6.7201 |
| \bar{E}' | 0.5591 | 0.6024 | 0.6687 | 0.8037 | 1.5049 | 3.1313 | 6.6942 |

The ground-state calculations were done in a bit modified way. Hamiltonian (25) is invariant with respect to the transformation $x \rightarrow -x$ again, which implies that the ground-state wave function is symmetrical. In such a situation it is possible to perform the calculation within the region $-L \leq x \leq 0$ with finite-element boundary conditions

$$\psi_{n1}(0,s) = \frac{\partial \psi_{nM}}{\partial x} \Big|_{x=h, \tau=s} = 0 \quad (26)$$

and to make the symmetric continuation to the region $0 \leq x \leq L$. The original scheme is then fully applicable. In this way it is possible to get a more accurate approximation at a given total number of spatial elements. The results are shown in Table V.

To determine the excited states of the system we have used the initial wave functions of the form

$$\psi_k(x,\alpha) = \left[\frac{2\alpha}{\pi} \right]^{1/2} \frac{1}{\sqrt{2^k k!}} H_k(\sqrt{2\alpha}x) \exp(-\alpha x^2) \quad (27)$$

with the value of α determined by minimizing the mean value of energy. $H_k(x)$ is the k th degree Hermitian polynomial, $k=1,2,\dots$. For $\alpha=0.5$ functions (27) are the excited-state wave functions of the corresponding har-

monic oscillator ($\lambda=0$). The numerical results are given in Table VI.

D. Ground state of the hydrogen atom

We have used the radial Schrödinger equation for the hydrogen atom with $l=0$ and determined the ground state of the system. The radial equation can be written in the form

$$\frac{\rho}{4} P - \rho^2 \frac{d^2 P}{d\rho^2} = \beta P, \quad (28)$$

where $P=P(\rho)$, $\beta=\beta(\bar{E})$. We have solved Eq. (5) with the Hamiltonian

$$\hat{H} = -\rho^2 \frac{d^2}{d\rho^2} + \frac{\rho}{4} \quad (29)$$

and $\rho > 0$. The numerical results are given in Table VII.

VI. CONCLUSIONS

We have used the steepest-descent method to compute the energies of the ground and excited states of simple quantum-mechanical systems. The calculations are performed using the finite-element method for solving the

TABLE VI. Ground and excited states of the anharmonic oscillator [Eq. (10)]. For a given value of the parameter λ the energy of the stationary state (\bar{E}) is shown and compared with the value given in the literature (\bar{E}')⁷. \bar{D} is the value of the variance in the resulting state.

| λ | 0.1 | 0.4 | 1.0 | 10 | 100 | 1000 |
|-------------|-----------------------|-----------------------|-----------------------|-----------------------|-----------------------|---------|
| 1 \bar{D} | 0.99×10^{-3} | 0.89×10^{-3} | 0.16×10^{-2} | 0.67×10^{-2} | 0.58×10^{-1} | 0.75 |
| \bar{E} | 0.5592 | 0.6688 | 0.8039 | 1.5050 | 3.1319 | 6.6998 |
| \bar{E}' | 0.5591 | 0.6687 | 0.8037 | 1.5049 | 3.13131 | 6.6942 |
| 2 \bar{D} | 0.18×10^{-1} | 0.17×10^{-1} | 0.19×10^{-1} | 0.64×10^{-1} | 1.07 | 0.61 |
| \bar{E} | 1.7724 | 2.2194 | 2.7382 | 5.3229 | 11.1977 | 23.9781 |
| \bar{E}' | 1.7694 | 2.2169 | 2.7378 | 5.3216 | 11.1873 | 28.9722 |
| 3 \bar{D} | 0.23×10^{-1} | 0.22×10^{-1} | 0.61×10^{-1} | 0.28 | 3.13 | 0.70 |
| \bar{E} | 3.1405 | 4.1070 | 5.1818 | 10.3500 | 21.940 | 47.020 |
| \bar{E}' | 3.1386 | 4.1028 | 5.1792 | 10.3471 | 21.906 | 47.017 |
| 4 \bar{D} | 0.72×10^{-1} | 0.61×10^{-1} | 0.50×10^{-1} | 1.74 | 6.45 | 2.58 |
| \bar{E} | 4.6339 | 6.2253 | 7.9482 | 16.150 | 34.09 | 73.45 |
| \bar{E}' | 4.6288 | 6.2155 | 7.9424 | 16.090 | 34.1825 | 73.4191 |

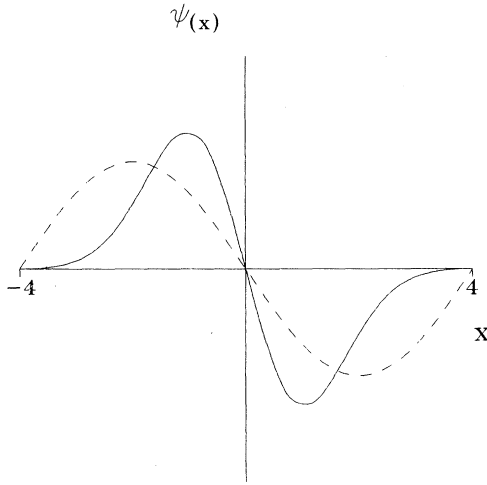


FIG. 4. The first excited state of the harmonic oscillator. The dashed line is the initial state (sinusoid) with corresponding energy $\bar{E}=2.569$. The solid line is the first excited state obtained after 25 time steps and its energy is $\bar{E}=1.501$ (exact value $\bar{E}=1.500$).

steepest-descent equations. The method gives very accurate results for both ground and excited states. We want to emphasize two specific properties of the scheme: its applicability to the excited-state calculations and the weak dependence on the choice of the trial wave function. From the computational point of view the scheme is simple and the numerical results are easy to obtain.

Because the norm of the wave function is preserved during the time evolution the method allows us to choose the time steps from the wide range of values. The method is based on solving the steepest-descent differential equations with specified initial and boundary conditions. The cases in which the boundary conditions need to be specified on both sides of the relevant region present no problem for the method, whereas such problems are known to be solvable only with considerable difficulty by standard methods.

Of course, the method can fail in some special cases. However, in such a situation one simply changes the size of the spatial region and the sizes of the time and spatial steps. The freedom to make these changes is rather large, so that the problem of divergences can be avoided effectively in practical cases.

To conclude, the steepest-descent method combined with the finite-element method is applicable and efficient

TABLE VII. Ground state of the hydrogen atom. L is the size of the spatial region and M is the number of spatial elements. Exact value: $\beta=1.0$.

| $L \backslash M$ | 10 | 15 | 20 | 25 |
|------------------|--------|--------|--------|--------|
| 10 | 1.0040 | 1.0038 | 1.0031 | 1.0026 |
| 14 | 1.0052 | 0.9965 | 0.9996 | 0.9998 |

in solving the quantum-mechanical problems. We hope that it can be used also in quantum field theory.

ACKNOWLEDGMENTS

Authors are indebted to J. Pišút, P. Prešnajder, and V. Černý for valuable discussions. Special thanks are due to J. Pišút, who has suggested many improvements of the original manuscript.

APPENDIX A

We shall describe here how the transition $\phi_n \rightarrow \phi_{n+1}$ was realized in practice. We shall discuss Eq. (9).

Having three conditions (i)–(iii) on each element we would obtain the consistent system of $3M$ equations determining the coefficients $\bar{a}_{nm}, \bar{b}_{nm}, \bar{c}_{nm}$, $m=1, 2, \dots, M$. However, it can be seen that for the first element conditions (i) and (iii) are absent. They are substituted by two boundary conditions (11). Suppose that the size L of the spatial region (see Fig. 1) is large enough, the discrete version of these conditions is

$$\psi_{n1}(0, s) = \psi_{n,M}(h, s) \quad (\text{A1})$$

or

$$\bar{c}_{n1} = 0, \quad (\text{A2})$$

$$\bar{a}_{nM} + \bar{b}_{nM} + \bar{c}_{nM} = 0. \quad (\text{A3})$$

After linearizing of Eq. (9) (see Sec. IV and Appendix B) all conditions are represented by the linear equations.

It can be seen that we have only two conditions (iii) and (A2) associated with the first element. This means that one of the coefficients $\bar{a}_{n1}, \bar{b}_{n1}, \bar{c}_{n1}$ remains free. If we choose \bar{a}_{n1} , then it is appropriate to introduce the parametrization

$$\begin{aligned} \bar{a}_{nm} &= \bar{a}_{nm}^1 + \bar{a}_{n1} \bar{a}_{nm}^2, \\ \bar{b}_{nm} &= \bar{b}_{nm}^1 + \bar{a}_{n1} \bar{b}_{nm}^2, \\ \bar{c}_{nm} &= \bar{c}_{nm}^1 + \bar{a}_{n1} \bar{c}_{nm}^2. \end{aligned} \quad (\text{A4})$$

In this way, each coefficient is specified by its two “components,” $\bar{a}_{nm} \equiv (\bar{a}_{nm}^1, \bar{a}_{nm}^2), \dots$. Using conditions (i)–(iii) we can then calculate successively these “components” up to the M th element. The boundary condition (A3) then gives

$$\bar{a}_{n1} = - \frac{\bar{a}_{nm}^1 + \bar{b}_{nm}^1 + \bar{c}_{nm}^1}{\bar{a}_{nm}^2 + \bar{b}_{nm}^2 + \bar{c}_{nm}^2}. \quad (\text{A5})$$

By repetitive substitutions into Eq. (A4) we will finally determine the coefficients.

As for Eq. (10), the strategy is quite analogous to the previous case. To have a consistent system of equations we have to complete the boundary conditions (A1) by those for the first derivative

$$\left. \frac{\partial \psi_{n1}}{\partial x} \right|_{x=0, \tau=s} = \left. \frac{\partial \psi_{nM}}{\partial x} \right|_{x=h, \tau=s} = 0. \quad (\text{A6})$$

In this case we will have two free coefficients, associated

with the first element. That is why it is necessary to do the double linear parametrization.

APPENDIX B

We shall describe here briefly the strategy which leads to the linearization of steepest-descent Eqs. (9) and (10).

The simplest approximation of Eq. (9) is the one with value $\bar{E}(\tau) = \bar{E}_0$ which corresponds to the first term in the expansion (16); i.e., the equation is

$$\frac{\partial \Psi}{\partial \tau} = -(\hat{H} - \bar{E}_0)\Psi \quad (\text{B1})$$

with $\bar{E}_0 = \int dx \phi_0 \hat{H} \phi_0$. It means that making the transition $\phi_n \rightarrow \phi_{n+1}$ we use this equation with $\bar{E}_0 = \int dx \phi_n \hat{H} \phi_n$. Maybe, this approximation seems to be too rough but our results presented above for the ground state were obtained just in this simple way. At the same time the convergence is very good. Making the time expansion of the solution of Eq. (B1) we can see the reason for that. The expansion is

$$\begin{aligned} \psi(x, \tau) = & \phi_0(x) + \tau(\bar{E}_0 - \hat{H})\phi_0(x) \\ & + \frac{\tau^2}{2}(\bar{E}_0 - \hat{H})^2\phi_0(x) + O(\tau^3). \end{aligned} \quad (\text{B2})$$

It differs from the expansion (15) of Eq. (9) only in the quadratic term. In addition, the difference of the coefficients at this term is proportional to \bar{D}_0 . Thus, when the state vector moves towards the ground state, Eq. (B1) becomes an increasingly better approximation to Eq. (9), because in this limit $\bar{D}_0 \rightarrow 0$. Taking into account the linear term in Eq. (16), we shall obtain the approximate equation, the solution of which differs only in cubic term from the expansion (15) of Eq. (9).

Making use of the expansions (15) and (B2) one can show in a straightforward way that the same improvement can be reached by making the transition $\phi_n \rightarrow \phi_{n+1}$ as follows.

In the first step Eq. (B1) is used to make the preliminary transition $\phi_n \rightarrow \phi'_{n+1}$. In the second step the real transition $\phi_n \rightarrow \phi_{n+1}$ is done by using the equation

$$\frac{\partial \Psi}{\partial \tau} = -(\hat{H} - \bar{E}'_0)\Psi \quad (\text{B3})$$

with $\bar{E}'_0 = \frac{1}{2}(\int \phi_n \hat{H} \phi_n + \int \phi'_{n+1} \hat{H} \phi'_{n+1})$.

As for Eq. (10) the situation is quite analogous. We have used the expansion (14) with linear term to express $\bar{E}(\tau), \bar{D}(\tau)$ through the initial state $\phi_0(x)$. The scheme described above works very well also.

¹C. M. Bender and D. H. Sharp, Phys. Rev. Lett. **50**, 1535 (1983); C. M. Bender, K. A. Milton, and D. H. Sharp, *ibid.* **51**, 1815 (1983); Phys. Rev. D **31**, 383 (1985).

²D. Horn and M. Weinstein, Phys. Rev. D **30**, 1256 (1984).

³A. Patkos and P. Rujan, J. Phys. A **18**, 1765 (1985).

⁴A. Duncan and R. Roskies, Phys. Rev. D **31**, 364 (1985).

⁵J. Ftáčnik, J. Pišút, V. Černý, and P. Prešnajder, Phys. Lett. A

116, 403 (1986); J. Ftáčnik, J. Pišút, and P. Prešnajder, Acta Phys. Slov. **37**, 275 (1987).

⁶G. Strang and G. J. Fix, *An Analysis of the Finite Element Method* (Prentice-Hall, Englewood Cliffs, NJ, 1973).

⁷F. T. Hioe, D. MacMillan, and E. W. Montroll, Phys. Rep. **43**, 305 (1978).